Phospholipase A_2 as a Target Protein for Nonsteroidal Anti-Inflammatory Drugs (NSAIDs): Crystal Structure of the Complex Formed between Phospholipase A_2 and Oxyphenbutazone at 1.6 Å Resolution†

Nagendra Singh, Talat Jabeen, Rishi K. Somvanshi, Sujata Sharma, Sharmistha Dey, and Tej P. Singh*

Department of Biophysics, All India Institute of Medical Sciences, New Delhi 110029, India

Received August 1, 2004; Revised Manuscript Received September 10, 2004

ABSTRACT: Phospholipase A_2 (PLA_2; EC 3.1.1.4) is a key enzyme involved in the production of proinflammatory mediators known as eicosanoids. The binding of the substrate to PLA_2 occurs through a well-formed hydrophobic channel. To determine the viability of PLA_2 as a target molecule for the structure-based drug design against inflammation, arthritis, and rheumatism, the crystal structure of the complex of PLA_2 with a known anti-inflammatory compound oxyphenbutazone (OPB), which has been determined at 1.6 Å resolution. The structure has been refined to an *R* factor of 0.209. The structure contains 1 molecule each of PLA_2 and OPB with 2 sulfate ions and 111 water molecules. The binding studies using surface plasmon resonance show that OPB binds to PLA_2 with a dissociation constant of 6.4×10^{-8} M. The structure determination has revealed the presence of an OPB molecule at the binding site of PLA_2. It fits well in the binding region, thus displaying a high level of complementarity. The structure also indicates that OPB works as a competitive inhibitor. A large number of hydrophobic interactions between the enzyme and the OPB molecule have been observed. The hydrophobic interactions involving residues Tyr^{52} and Lys^{69} with OPB are particularly noteworthy. Other residues of the hydrophobic channel such as Leu^3, Phe^5, Met^8, Ile^9, and Ala^{18} are also interacting extensively with the inhibitor. The crystal structure clearly reveals that the binding of OPB to PLA_2 is specific in nature and possibly suggests that the basis of its anti-inflammatory effects may be due to its binding to PLA_2 as well.

Phospholipase A_2 (PLA_2;[1] EC 3.1.1.4) hydrolyzes the membrane phospholipids to release free fatty acids. It specifically hydrolyzes the *sn*-2 acyl bond of phospholipids and produces equimolar amounts of lysophospholipids and free fatty acids. This forms the first step of a cascade reaction involving several enzymes, which produce a group of proinflammatory lipid mediators, known as eicosanoids (*1*). It has been reported that extremely high levels of PLA_2 were observed in synovial fluid from the inflammatory conditions of joints of arthritic patients, which suggested that PLA_2 may also be responsible for the state of inflammation (*2*, *3*). It has also been shown that the architectures of binding sites and the binding mechanisms of inhibitors in both human and snake venom PLA_2 are similar (*4*). In view of this, PLA_2 may also form a potential target for the design of anti-inflammatory agents. To design specific anti-inflammatory agents using PLA_2 as a target molecule, it is highly desirable to obtain the detailed structural information of various complexes of PLA_2 with known nonsteroidal anti-inflammatory drugs (NSAIDs). The structures of PLA_2s from a number of sources belonging to different classes and isoforms are already known (*5*−*22*). Prior to the availability of structures of PLA_2s and those of several other enzymes of the cascade reaction, many compounds were in use as anti-inflammatory agents. However, the mode of their bindings and the sites of binding in the target enzymes were not clearly described. These compounds were developed using conventional methods based on certain available leads. The information about the role of PLA_2 in the resulting anti-inflammatory effects of NSAIDs was also not available. Thus, the binding studies of NSAIDs with PLA_2 and the details of their interactions at the atomic level will be helpful for the design of new and more potent anti-inflammatory agents. Therefore, the structure of the complex formed between a group II PLA_2 (Russell's viper) and a known anti-inflammatory agent oxyphenbutazone (OPB) has been determined at 1.6 Å resolution. This compound is predominantly hydrophobic in nature and possesses both rigid and flexible moieties (*23*, *24*). The structure of the complex reveals that OPB binds to PLA_2 at the substrate-binding site and forms several attractive intermolecular interactions. The native conformation of PLA_2 does not change appreciably but that of OPB changes significantly upon complex formation, thus indicating a good induced fit in OPB upon binding to PLA_2. The results of these investigations are expected to

† Supported by the Department of Science and Technology (DST), New Delhi, under the Funds for Improvement of S&T infrastructure in universities and other higher educational institutions (FIST) program.

* To whom correspondence should be addressed: Department of Biophysics, All India Institute of Medical Sciences, Ansari Nagar, New Delhi 110 029, India. Telephone: +91-11-2658-8931. Fax: +91-11-2658-8663. E-mail: tps@aiims.aiims.ac.in.

[1] Abbreviations: DLS, dynamic light scattering; MALDI−TOF, matrix-assisted laser desorption ionization time of flight; NSAIDs, nonsteroidal anti-inflammatory drugs; OPB, oxyphenbutazone; PDB, Protein Data Bank; PLA_2, phospholipase A_2; rms, root mean square; SDS−PAGE, sodium dodecyl sulphate−polyacrylamide gel electrophoresis; SPR, surface plasmon resonance.

10.1021/bi0483561 CCC: $27.50
Published on Web 10/30/2004

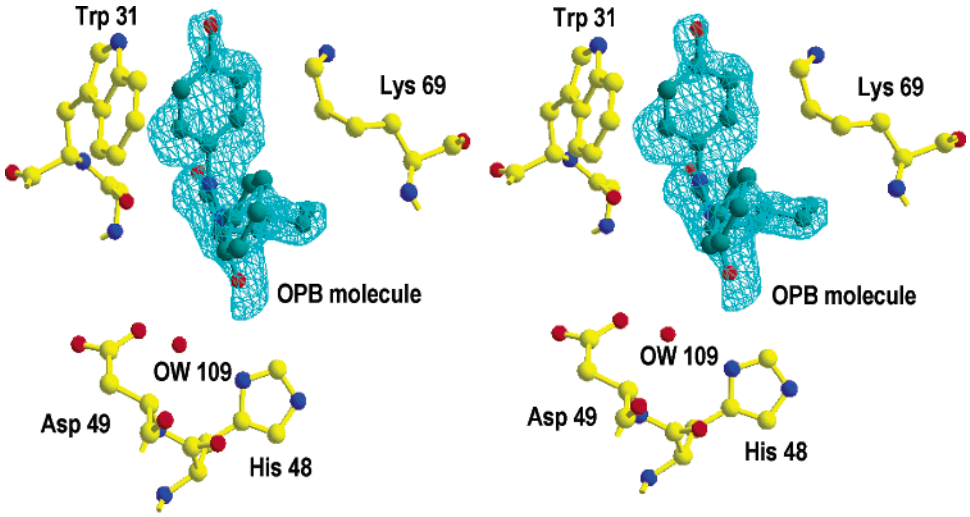

FIGURE 1: Stereoview of the ($F_o - F_c$) map contoured at 2.5σ showing the electron density for the 4-butyl-1-(4-hydroxyphenyl)-2-phenyl-3,5-pyrazolidinedione molecule (OPB).

Table 1: Data Collection Statistics

space group	$P4_1/P4_3$
cell dimensions (Å)	
$a = b$	53.0
c	48.2
Z	4
Matthews coefficient (V_m) (Å^3/Da)	2.5
solvent content (%)	50
resolution range (Å)	20.0−1.6
highest resolution shell (Å)	1.65−1.60
total number of reflections	80 517
number of unique reflections	15 926
overall completeness (%)	99.8
completeness in the highest resolution shell (%)	95.0
overall R_{sym} (%)	7.3
R_{sym} in the highest resolution shell (%)	21.8
mean overall $I/\sigma(I)$	23
mean $I/\sigma(I)$ in the highest resolution shell	2.5

Table 2: Refinement Statistics

PDB code	1Q7A
space group	$P4_3$
resolutions limits (Å)	20.0−1.6
number of reflections	15 926
R_{cryst} (%)	20.9
R_{free} (%)	21.3
number of protein atoms	944
number of oxyphenbutazone atoms	24
number of sulfate ions	2
number of methanol molecule	1
number of water molecules	111
rms deviations from ideal values	
bond lengths (Å)	0.007
bond angles (deg)	1.4
dihedral angles (deg)	22.7
average B factors (Å^2)	
from Wilson plot	25.3
main chain atoms	27.5
side chains, water molecules, and oxyphenbutazone atoms	32.4
for all atoms	30.2
Ramachandran plot	
residues in the most allowed regions (%)	92.2
residues in the additionally allowed region (%)	7.8

guide in identifying the new interactions that may be important in further molecular recognition so that an improvement in the design of inhibitors can be made.

MATERIALS AND METHODS

Purification of the Protein. The crude venom of *Daboia russelli pulchella* was obtained from the Irula Cooperative Snake Farm in Tamil Nadu, India. A total of 250 mg of the lyophilized venom was dissolved in 50 mM ammonium acetate buffer at pH 6.0, to make the final concentration of venom to 10 mg/mL. The solution was centrifuged at 20 000 rpm for 15 min at 293 K. The insoluble material was removed, and the supernatant was diluted 3 times with the same buffer. This was loaded on a Cibacron blue affinity column (30 × 2.5 cm). The bound venom fractions were eluted first with 50 mM ammonium bicarbonate buffer at pH 8.0 and then using 20 mM ammonium carbonate buffer at pH 10.5. The fractions collected at pH 10.5 were pooled and concentrated. The sample was loaded on a CM Sephadex cation exchanger column (30 × 2.5 cm). The bound protein fractions were eluted using 0−0.5 M gradient of NaCl in 50 mM ammonium acetate buffer at pH 6.0. The eluted fractions showed PLA_2 activity and were collected and desalted. This was analyzed on sodium dodecyl sulfate−polyacrylamide gel electrophoresis (SDS−PAGE) and matrix-assisted laser desorption ionization time of flight (MALDI−TOF) (Kratos, Shimadzu, Japan). To further confirm the identity of the protein, the N-terminal sequence of the first 15 residues was also determined using the protein sequencer PPSQ 21 (Shimadzu, Japan).

Binding Studies of OPB. The binding studies were carried out using the BIACore 2000 apparatus (Pharmacia BIACore AB, Uppsala, Sweden). The BIACore apparatus is a biosensor-based system for real-time-specific interaction analysis (*25*). The sensor chips CM5, surfactant P20, amine-coupling kit containing *N*-hydroxysuccinimide (NHS), *N*-ethyl-*N*′-3 (diethylaminopropyl) carbodiimide (EDC), and ethanolamine hydrochloride were used. The running buffer used was 5 mM HEPES (pH 7.4) and 0.005% surfactant P20. The immobilization of PLA_2 was performed at a flow rate of 10 μL/min at 25 °C. The dextran on the chip was equilibrated with a running buffer, and the carbomethylated matrix was activated with an EDC/NHS mixture. A total of 210 μL of PLA_2 (50 μg/mL) in 10 mM sodium acetate (pH 4.8) was injected, and unreacted groups were blocked by injection of ethanolamine (pH 8.5). The SPR signal for immobilized PLA_2 was found to be 5049 RUs.

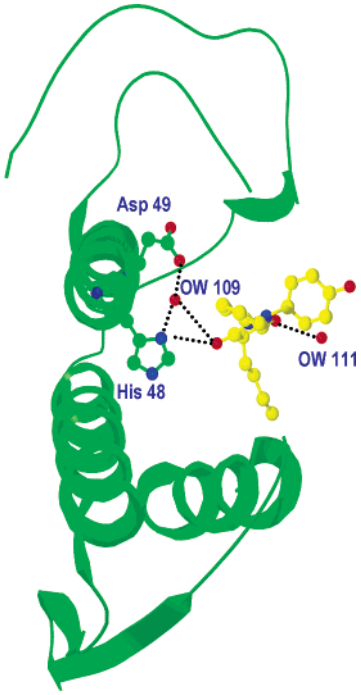

FIGURE 2: Structure of the complex of PLA_2 with OPB showing its placement at the binding site of PLA_2.

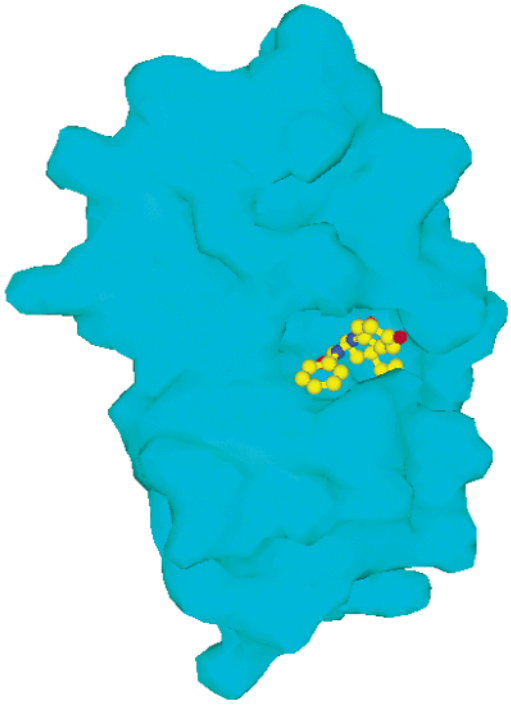

FIGURE 4: GRASP (*39*) representation of PLA_2 showing the binding cavity with the OPB molecule (ball and stick) in the binding pocket.

Crystallization. The OPB was dissolved in deionized water containing 5 mM $CaCl_2$ and 30% methanol to a concentration of 15 mg/mL. The purified protein was dissolved in the above solution to make a final concentration of the protein to 10 mg/mL. Crystallization was carried out using the hanging-drop vapor-diffusion method at 293 K in 24-well plates. The protein drops of 10 μL were equilibrated against the reservoir solution containing 0.2 M $(NH_4)_2SO_4$ and 30% PEG 4000 in the deionized water. The crystals measuring to the dimensions of $0.25 \times 0.21 \times 0.18$ mm^3 grew in 6 weeks.

X-ray Intensity Data Collection. High-resolution X-ray diffraction intensity data were collected at 287 K using a MAR Research 345-mm imaging plate scanner mounted on a rotating anode X-ray generator RU-300 (Rigaku, Japan), which is equipped with Osmic mirrors. The data were processed with DENZO and SCALEPACK from the HKL package (*26*). It gave a data set with 99.8% completeness to 1.6 Å resolution (Table 1). The space group was either $P4_1$ or $P4_3$, with unit cell parameters of $a = b = 53.0$ Å and $c = 48.2$ Å. The packing density for one PLA_2−OPB complex molecule in the asymmetric unit of these crystals was 2.5 $Å^3$ Da^{-1}, corresponding to an approximate solvent content of 50%, a reasonable value for globular proteins (*27*).

Structure Determination and Refinement. The crystal structure of the complex of PLA_2 with OPB was determined with molecular replacement using AMoRe (*28*). The coordinates of one molecule from the dimer of PLA_2 from *Daboia russelli pulchella* (*11*; 1FB2) were used to build the initial search model. The top peak in both the rotation and translation functions gave the best solution in the correct space group $P4_3$. The solution was further improved with

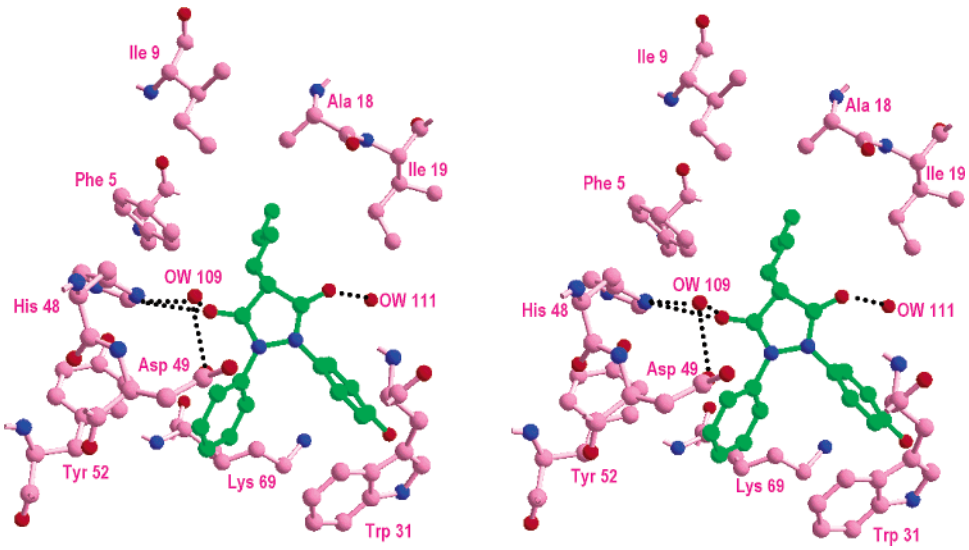

FIGURE 3: Stereoview of OPB (green) in the hydrophobic environment of the binding site of PLA_2. The residues involved in the interactions are drawn (pink).

Table 3: Hydrogen Bonds and van der Waals Contact Distances ≤4.35 Å between PLA_2 and OPB Molecules

OPB	PLA_2/water molecules	distance (Å)
O1	His^{48} (Nδ1)	3.38
	OW^{109}	3.38
O2	OW^{111}	3.12
OH	Asn^{111} (O)*	2.66
C7	Phe^{5} (Cε2)	3.74
	Phe^{5} (Cδ2)	3.43
C8	Ile^{9} (Cδ1)	4.17
	Ala^{18} (Cβ)	4.09
C9	Leu^{2} (Cγ)	4.26
	Phe^{5} (Cδ2)	3.84
C10	Ala^{18} (Cβ)	3.24
	Gly^{6} (Cα)	3.42
	Ile^{19} (Cγ1)	4.29
C12	Tyr^{52} Cδ2)	3.81
	Tyr^{52} (Cε2)	3.77
C13	Tyr^{52} (Cδ2)	2.98
	Tyr^{52} (Cε2)	3.14
C14	Lys^{69} (Cγ)	4.30
C15	Lys^{69} (Cδ)	3.27
	Lys^{69} (Cγ)	3.23
C16	Leu^{2} (Cδ2)	3.63
	Lys^{69} (Cδ)	3.87
C18	Leu^{2} (Cδ2)	3.52
C19	Leu^{2} (Cδ2)	3.91
C21	Trp^{31} (Cδ1)	3.35
	Trp^{31} (Cζ2)	4.35
	Trp^{31} (Cε2)	3.57
	Trp^{31} (Cδ2)	3.57

rigid-body refinement that gave a correlation coefficient of 60.2% and an *R* factor of 43.1%.

Manual fitting of the model to the electron density was carried out using the program "O" (*29*). A total of 4.9% of the reflections were randomly selected to create a data set of test reflections for cross validation of the refinement procedure. The structure was refined in the resolution range of 20.0−1.6 Å initially with X-PLOR (*30*), using protocols for rigid-body refinement, slow-cooling simulated annealing, and minimization. The final steps of refinement were carried out with CNS (*31*; using torsion molecular dynamics, slow-cooling simulated annealing, maximum-likelihood target function, energy minimization, and individual *B*-factor refinement). After these steps, the *R* and R_{free} factors dropped to 0.246 and 0.281, respectively. At this stage, a very characteristic continuous electron density was observed at the binding site of PLA_2. Using the coordinates of OPB reported by Krishnamurthy and Vijayan (*23*), it was fitted into the difference Fourier map at a 2.0σ cut off (Figure 1). The coordinates of OPB thus fitted were included in the further steps of refinement. The positions of 111 water molecules were identified from the difference Fourier ($F_o - F_c$) maps and were checked manually for their interactions with protein atoms. In addition, two sulfate ions and one methanol molecule were also observed and included in the subsequent refinement cycles. The R_{cryst} factor of the final model is 0.209, and the R_{free} factor is 0.213. The crystallographic refinement statistics are given in Table 2.

RESULTS AND DISCUSSION

Inhibition of PLA_2 by OPB. The purified samples of PLA_2 showed a molecular weight of 14 kDa on SDS−PAGE. The measurement of hydrodynamic radius (R_H) using dynamic light scattering (DLS) also indicated a molecular weight of approximately 14 kDa. The association of OPB to immobilized PLA_2 was studied by injecting at 25 °C, 50, 75, 100, 125, and 150 μg/mL separately at different cycles in 50 mM HEPES (pH 7.4) with 5 mM Ca^{2+} at a flow rate of 10 μg/mL. The dissociation of OPB was performed by 50 mM HEPES (pH 7.4). Regeneration of the immobilized protein was performed using 10 mM glycine-HCl buffer (pH 2.5). The analysis was carried out using BIA evaluation software (Pharmacia BIACore) (*32*). The dissociation constant (K_d) was calculated to be 6.4×10^{-8} M. This interaction strength is expected to allow association of OPB *in vivo*.

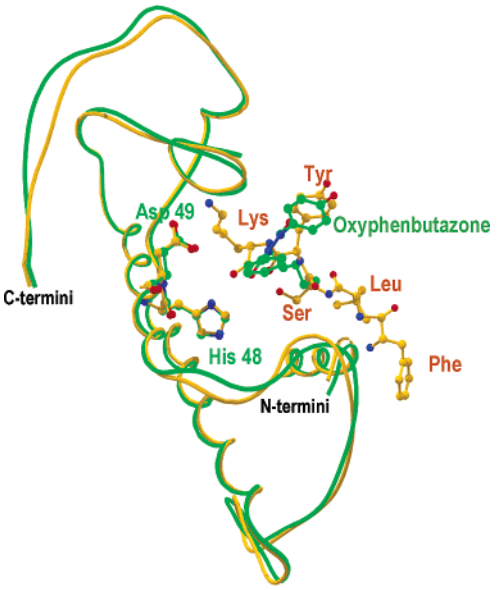

FIGURE 5: Superimposition of the PLA_2−OPB complex (green) on the PLA_2−FLSYK complex (yellow) (*38*). The OPB molecule overlaps well with the middle part of the peptide.

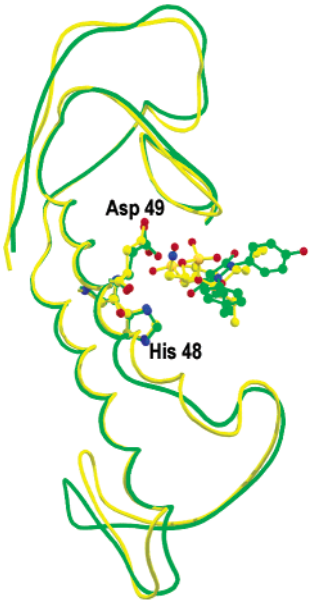

FIGURE 6: Superimposition of the PLA_2−OPB complex on the human PLA_2−transition-state analogue complex (*10*), showing similar binding space for the ligands.

Quality of the Model. The final model consists of a monomer of PLA_2, 1 molecule of OPB, 2 sulfate ions, 1 molecule of methanol, and 111 water molecules. The refinement of the final model converged to $R_{cryst} = 20.9\%$ and $R_{free} = 21.3\%$ for 15 926 reflections in the resolution range of 20.0−1.6 Å. The model had a good geometry with

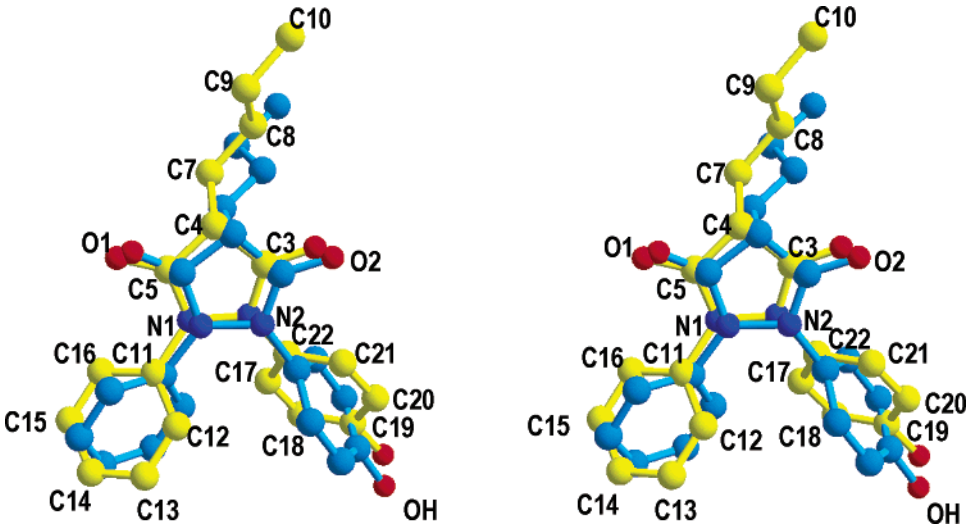

FIGURE 7: Superimposition of the OPB molecule in the complex (blue) on the free molecule (yellow) (*23*).

root-mean-square (rms) deviations of 0.007 Å and 1.4° for bond lengths and angles, respectively. The Ramachandran plot (*33*) obtained with PROCHECK (*34*) showed that 92.2% of the dihedral angles were found in the most favored regions, while the remaining 7.8% of residues were present in the additionally allowed regions. The average *B* value for all of the atoms was 30.2 $Å^2$.

Binding of OPB to PLA_2. The high quality of electron density for OPB in the ($F_o - F_c$) map allowed an accurate determination of its atomic coordinates. The OPB molecule was clearly located in the center of the hydrophobic channel, and it fitted well with respect to the binding site of the enzyme (Figure 2). The O1 atom of OPB molecule formed a hydrogen bond with OW^{109}, which in turn interacted with His^{48} and Asp^{49} simultaneously. The second oxygen atom O2 formed a hydrogen bond with another water molecule OW^{111}. It also formed a number of hydrophobic interactions with the residues of the channel (Figure 3). In fact, it appeared completely buried in the binding cleft of the enzyme (Figure 4). The most notable interactions were observed with Leu^2, Phe^5, Ile^9, Tyr^{52}, and Lys^{69} (Table 3). Almost all of the residues of the hydrophobic channel participated in the interactions with OPB (Figure 3 and Table 3). The initial degree of complimentarity between the shape of the binding site and that of the OPB molecule was high, which appeared to have further improved upon binding. So far, four other structures of the complexes of PLA_2 from the venom of *Daboia russelli pulchella* with natural compounds, vitamin E (*35*) and aristolochic acid (*36*), and designed peptide inhibitors, Leu-Ala-Ile-Tyr-Ser (*37*) and Phe-Leu-Ser-Tyr-Lys (*38*) have been determined. A comparison of the present complex with the above complexes shows an excellant overlap of the OPB molecule with ligands in these structures (*35*−*38*). As shown in Figure 5, the OPB molecule occupies an identical space as occupied by the middle portion of one of the most potent peptide inhibitors FLSYK in the complex with PLA_2 (*38*; 1JQ9). A further comparison of the structure of present complex with that of the complex of human PLA_2 with a substrate analogue inhibitor shows that the OPB molecule covers a major portion in the hydrophobic substrate-binding site of PLA_2 as covered by the substrate analogue inhibitor, thus indicating the use of the same binding site by the OPB molecule (Figure 6). It may be mentioned here that

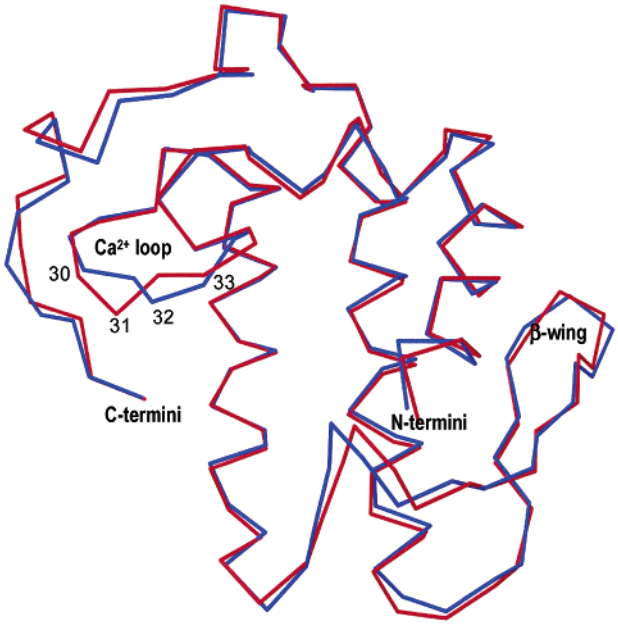

FIGURE 8: Superimposition of C^α traces of PLA_2 from the present complex (red) on the native PLA_2 molecule (blue) (*11*).

the OPB molecule contains a 3,5-pyrazolidinedione ring having substitutions at 1, 2, and 4 positions with three different chemical moieties. At positions 1 and 2, it has aromatic benzene and hydroxyphenyl rings respectively, while at position 4, a flexible *n*-butyl group is present. The aromatic rings are capable of undergoing rotations about N1−C11 and N2−C17 bonds. While the butyl group is flexible as a whole. As seen from Figure 7, the orientations of phenolic and butyl groups of OPB in the complex are significantly different than those observed in the free OPB structure (23). The planes of two aromatic rings in the complex have rotated by 90.0° and 104.6° with respect to the planes of benzene and hydroxyphenyl rings of the OPB molecule. Similarly, the atoms of the butyl group have shifted considerably from the corresponding atoms in the free OPB molecule. The inherent flexibility and strongly hydrophobic nature of the OPB molecule were its favorable properties for interactions with the PLA_2 enzyme as an inhibitor.

Overall PLA_2 Structure. The overall structure of PLA_2 in the present complex is essentially similar to that reported

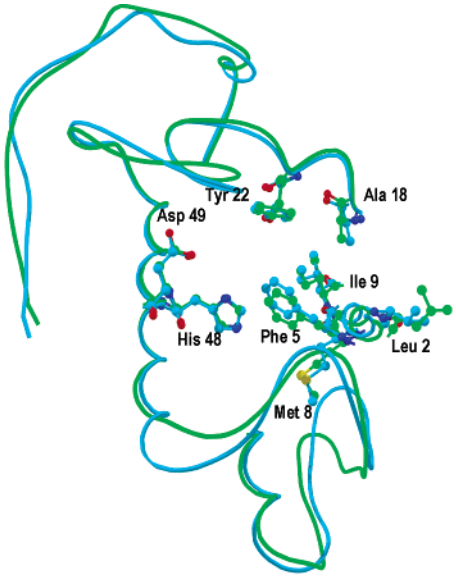

FIGURE 9: Superimposition of PLA_2 from the present complex (green) on human native PLA_2 (blue) (*14*). The side chains of important residues of the hydrophobic substrate-binding site that are involved in the recognition have also been indicated.

earlier in the native state (*11*). The superposition of the C^{α} chains of two structures shows an rms shift of 0.70 Å. The only notable conformational variation was observed in the folding of the calcium-binding loop (Figure 8). The calcium-binding loop constitutes one of the walls of the substrate-binding hydrophobic channel, and hence, the rearrangement of the flexible calcium-binding loop can occur to accommodate the OPB molecule. It has been shown that the Russell's PLA_2 does not require calcium ion for its activity (*11*). The structure of the present venom PLA_2 is also very similar to the human synovial PLA_2 (*14*), having an rms shift of 0.82 Å for their C^{α} positions. The side chains of the residues of the active sites in the two structures occupy nearly identical positions. Although there are a few sequence differences among the residues that constitute the substrate-recognition hydrophobic channel, but the residues that participate in the recognition of ligands are almost identical except Leu^3 (Val in human PLA_2) and Ile^{19} (Leu in human PLA_2). As seen from Figure 9, most of the side chains of hydrophobic channel that are expected to interact with a substrate/inhibitor are oriented in a similar way.

CONCLUSIONS

The structure of the complex formed between PLA_2 and an old NSAID OPB demonstrates that the drug molecule binds to PLA_2 at the substrate-recognition site in the hydrophobic channel and interacts with the catalytic residues His^{48} and Asp^{49}. The OPB molecule is almost completely buried in the core of the hydrophobic channel and makes a number of van der Waals contacts with the residues located on the side of the hydrophobic channel. Upon binding to PLA_2, the OPB molecule undergoes significant conformational changes, while the structure of PLA_2 is not appreciably perturbed except for small changes in the calcium-binding loop. The high degree of conformational compatibility of the OPB molecule with that of the substrate-binding region is reflected in the form of a high dissociation constant of 6.4×10^{-8} M. This interaction strength will allow the OPB molecule to bind to the PLA_2 enzyme effectively *in vivo* conditions as well. The underlying idea behind the determination of the crystal structure of the present complex of PLA_2 with the OPB molecule has been to understand the mode of binding and its precise structure when bound to PLA_2. This information will be used for constructing new molecules with improved potency. The repeated cycles of the combinations of structure analysis, synthesis of new compounds, and binding studies are required for a rational structure-based drug design.

ACKNOWLEDGMENT

N. S. and T. J. thank the Council of Scientific and Industrial Research (CSIR), New Delhi, for the award of fellowships.

REFERENCES

1. Smith, W. L. (1992) Prostanoid biosynthesis and mechanisms of action, *Am. J. Physiol. 263*, F181−F191.
2. . Pruzanski, W., Bogoch, E., Stefanski, E., Wloch, M., and Vadas, P. (1991) Enzymatic activity and distribution of phospholipase A_2 in human cartilage, *Life Sci. 48*, 2457−2462.
3. Vadas, P., Pruzanski, W., Kim, J., and Fornasier, V. (1989) The pro-inflammatory effect of intra-articular injection of soluble human and venom phospholipase A_2, *Am. J. Pathol. 134*, 807−811.
4. Dennis, E. A. (1994) Diversity of group types, regulation, and function of phospholipase A_2, *J. Biol. Chem. 269*, 13057−13060.
5. Scott, D. L., Otwinowski, Z., Gelb, M. H., and Sigler, P. B. (1990) Crystal structure of bee-venom phospholipase A_2 in a complex with a transition-state analogue, *Science 250*, 1563−1566.
6. Thunnissen, M. M. G. M., Eiso, A. B., Kalk, K. H., Drenth, J., Dijkstra, B. W., Kuipers, O. P., Dijkman, R., de Haas, G. H., and Verheij, H. M. (1990) X-ray structure of phospholipase A_2 complexed with a substrate-derived inhibitor, *Nature 347*, 689−691.
7. Westerlund, B., Nordlund, P., Uhlin, U., Eaker, D., and Eklund, H. (1992) The three-dimensional structure of notexin, a presynaptic neurotoxic phospholipase A_2 at 2.0 Å resolution, *FEBS Lett. 301*, 159−164.
8. Kudo, I., Murakami, M., Hara, S., and Inoue, K. (1993) Mammalian non-pancreatic phospholipases A_2, *Biochim. Biophys. Acta 1170*, 217−231.
9. Arni, R. K., Fontes, M. R., Barberato, C., Gutierrez, J. M., Diaz, C., and Ward, R. J. (1999) Crystal structure of myotoxin II, a monomeric Lys^{49}-phospholipase A_2 homologue isolated from the venom of *Cerrophidion (Bothrops) godmani*, *Arch. Biochem. Biophys. 366*, 177−182.
10. Scott, D. L., White, S. P., Browning, J. L., Rosa, J. J., Gelb, M. H., and Sigler, P. B. (1991) Structures of free and inhibited human secretory phospholipase A_2 from inflammatory exudate, *Science 254*, 1007−1010.
11. Chandra, V., Kaur, P., Jasti, J., Betzel, C., and Singh, T. P. (2001) Regulation of catalytic function by molecular association: Structure of phospholipase A_2 from *Daboia russelli pulchella* ($DPLA_2$) at 1.9 Å resolution, *Acta Crystallogr., Sect. D 57*, 1793−1797.
12. Tang, L., Zhou, Y. C., and Lin, Z. J. (1998) Crystal structure of agkistrodotoxin, a phospholipase A_2-type presynaptic neurotoxin from *Agkistrodon halys pallas*, *J. Mol. Biol. 282*, 1−11.
13. Segelke, B. W., Nguyen, D., Chee, R., Xuong, N. H., and Dennis, E. A. (1998) Structures of two novel crystal forms of *Naja naja naja* phospholipase A_2 lacking Ca^{2+} reveal trimeric packing, *J. Mol. Biol. 279*, 223−232.
14. Wery, J. P., Schevitz, R. W., Clawson, D. K., Bobbitt, J. L., Dow, E. R., Gamboa, G., Goodson, T., Jr., Hermann, R. B., Kramer, R. M., McClure, D. B., et al. (1991) Structure of recombinant human rheumatoid arthritic synovial fluid phospholipase A_2 at 2.2 Å resolution, *Nature 352*, 79−82.
15. Dijkstra, B. W., Kalk, K. H., Hol, W. G., and Drenth, J. (1981) Structure of bovine pancreatic phospholipase A_2 at 1.7 Å resolution, *J. Mol. Biol. 147*, 97−123.
16. Singh, G., Gourinath, S., Sharma, S., Paramasivam, M., Srinivasan, A., and Singh, T. P. (2001) Sequence and crystal structure

determination of a basic phospholipase A_2 from common krait (*Bungarus caeruleus*) at 2.4 Å resolution: Identification and characterization of its pharmacological sites, *J. Mol. Biol. 307*, 1049−1059.
17. Finzel, B. C., Ohlendorf, D. H., Weber, P. C., and Salemme, F. R. (1991) An independent crystallographic refinement of porcine phospholipase A_2 at 2.4 Å resolution, *Acta Crystallogr., Sect. B 47*, 558−559.
18. Banumathi, S., Rajashankar, K. R., Notzel, C., Aleksiev, B., Singh, T. P., Genov, N., and Betzel, C. (2001) Structure of the neurotoxic complex vipoxin at 1.4 Å resolution, *Acta Crystallogr., Sect. D 57*, 1552−1559.
19. Pan, Y. H., Yu, B. Z., Singer, A. G., Ghomashchi, F., Lambeau, G., Gelb, M. H., Jain, M. K., and Bahnson, B. J. (2002) Crystal structure of human group X secreted phospholipase A_2. Electrostatically neutral interfacial surface targets zwitterionic membranes, *J. Biol. Chem. 277*, 29086−29093.
20. Perisic, O., Fong, S., Lynch, D. E., Bycroft, M., and Williams, R. L. (1998) Crystal structure of a calcium-phospholipid binding domain from cytosolic phospholipase A_2, *J. Biol. Chem. 273*, 1596−1604.
21. Carredano, E., Westerlund, B., Persson, B., Saarinen, M., Ramaswamy, S., Eaker, D., and Eklund, H. (1998) The three-dimensional structures of two toxins from snake venom throw light on the anticoagulant and neurotoxic sites of phospholipase A_2, *Toxicon 36*, 75−92.
22. Steiner, R. A., Rozeboom, H. J., de Vries, A., Kalk, K. H., Murshudov, G. N., Wilson, K. S., and Dijkstra, B. W. (2001) X-ray structure of bovine pancreatic phospholipase A_2 at atomic resolution, *Acta Crystallogr., Sect. D 57*, 516−526.
23. Krishnamurthy, H. M., and Vijayan, M. (1981) Structural studies of analgesics and their interactions. Part VII. Stereoisomerism and disorder in the structure of oxyphenbutazone monohydrate, *Acta Crystallogr., Sect. B 37*, 210−213.
24. Singh, T. P., and Vijayan, M. (1977) Structural studies of analgesics and their interactions. Part IV: Crystal and molecular structures of phenylbutazone and a 2:1 complex with piperazine, *J. Chem. Soc.* (Parkin II), 693−701.
25. Szabo, A., Stolz, L., and Granzow, R. (1995) Surface plasmon resonance and its use in biomolecular interaction analysis (BIA), *Curr. Opin. Struct. Biol. 5*, 699−705.
26. Otwinowski, Z., and Minor, W. (1997) Processing of X-ray diffraction data collected in oscillation mode, *Methods Enzymol. 276*, 307−325.
27. Matthews, B. W. (1968) Solvent content of protein crystals, *J. Mol. Biol.* 33, 491−497.
28. Navaza, J. (1994) AMoRe: An automated package for molecular replacement, *Acta Crystallogr., Sect. A 50*, 157−163.
29. Jones, T. A., Zou, J., Cowan, S. W., and Kjeldgaard, M. (1991) Improved methods for building models in electron density maps and the location of errors in these models, *Acta Crystallogr., Sect. A 47*, 110−118.
30. Brünger, A. T. (1992) The free *R* value: A novel statistical quantity for assessing the accuracy of crystal structures, *Nature 355*, 472−474.
31. Brünger, A. T., Adams, P. D., Clore, G. M., DeLano, W. L., Gros, P., Grosse-Kunstleve, R. W., Jiang, J. S., Kuszewski, J., Nilges, M., Pannu, N. S., Read, R. J., Rice, L. M., Simonson, T., and Warren, G. L. (1998) Crystallography and NMR system: A new software suite for macromolecular structure determination, *Acta Crystallogr., Sect. D 54*, 905−921.
32. Nieba, L., Krebber, A., and Plückhun, A. (1996) Competition BIAcore for measuring true affinities: Large differences from values determined from binding kinetics, *Anal. Biochem. 234*, 155−165.
33. Ramachandran, G. N., and Sasisekharan, V. (1968) Conformation of polypeptides and proteins, *Adv. Protein Chem. 23*, 283−438.
34. Laskowski, R., Macarthur, M., Moss, D., and Thornton, J. (1993) Procheck: A program to check stereochemical quality of protein structures, *J. Appl. Crystallogr. 26*, 283−290.
35. Chandra, V., Jasti, J., Kaur, P., Srinivasan, A., Betzel, C., and Singh, T. P. (2002) First structural evidence of a specific inhibition of phospholipase A_2 by α-tocopherol (vitamin E) and its implications in inflammation: Crystal structure of the complex formed between phospholipase A_2 and α-tocopherol at 1.8 Å resolution, *Acta Crystallogr., Sect. D 58*, 1813−1819.
36. Chandra, V., Jasti, J., Kaur, P. Betzel, C., and Singh, T. P. (2002) Structural basis of phospholipase A_2 inhibition for the synthesis of prostaglandins by the plant alkaloid aristolochic acid from a 1.7 Å crystal structure, *Biochemistry 41*, 10914−10919.
37. Chandra, V., Jasti, J., Kaur, P., Dey, S., Perbandt, M., Srinivasan, A., Betzel, C., and Singh, T. P. (2002) Design of specific inhibitors of phospholipase A_2: Structure of a complex formed between a Russelli viper phospholipase A_2 and a designed peptide Leu-Ala-Ile-Tyr-Ser, *Acta Crystallogr., Sect. D 58*, 1813−1819.
38. Chandra, V., Jasti, J., Kaur, P., Dey, S., Perbandt, M., Srinivasan, A., Betzel, C., and Singh, T. P. (2002) Crystal structure of a complex formed between a snake venom phospholipase A_2 and a potent peptide inhibitor Phe-Leu-Ser-Tyr-Lys at 1.8 Å resolution, *J. Biol. Chem. 277*, 41079−41085.
39. Nicholls, A., Sharp, K. A., and Honig, B. (1991) Protein folding and association: Insights from the interfacial and thermodynamic properties of hydrocarbons, *Proteins 11*, 281−296.

BI0483561